

On the Combined Analysis of Muon Shower Size and Depth of Shower Maximum

Jakub Vicha*, **Petr Trávníček**

*Institute of Physics of the Academy of Sciences of the Czech Republic,
Na Slovance 2, 182 21 Prague 8
E-mail: vicha@fzu.cz*

Dalibor Nosek

*Faculty of Mathematics and Physics, Charles University in Prague,
V Holešovičkách 2, 180 00 Prague 8*

The mass composition of ultra-high energy cosmic rays can be studied from the distributions of the depth of shower maximum and/or the muon shower size. Here, we study the dependence of the mean muon shower size on the depth of shower maximum in detail. Air showers induced by protons and iron nuclei were simulated with two models of hadronic interactions already tuned with LHC data (run I-II). The generated air showers were combined to obtain various types of mass composition of the primary beam. We investigated the shape of the functional dependence of the mean muon shower size on the depth of shower maximum and its dependency on the composition mixture. Fitting this dependence we can derive the primary fractions and the muon rescaling factor with a statistical uncertainty at a level of few percent. The difference between the reconstructed primary fractions is below 20% when different models are considered. The difference in the muon shower size between the two models was observed to be around 6%.

*The 34th International Cosmic Ray Conference,
30 July - 6 August, 2015
The Hague, The Netherlands*

*Speaker.

1. Introduction

The mass composition of ultra-high energy cosmic rays (UHECR) inducing extensive air showers of energies above 10^{18} eV can be measured by fluorescence detectors on average basis. The measurement of the depth of shower maximum (X_{\max}) is compared with Monte Carlo (MC) predictions in such cases [1, 2]. The fluorescence technique provides a precise measurement of X_{\max} , but a large systematic uncertainty remains in the determination of the mass composition of UHECR. The obstacle comes predominantly from different predictions of hadronic interaction models that are extrapolated from accelerator energies to energies larger by a few orders of magnitude in the center of mass system. The mass composition of UHECR remains uncertain, and even unknown at the highest energies where a steep decrease of the flux is observed [3, 4]. The very low statistics of events collected by fluorescence detectors is due to their low duty cycle.

Assuming a small number of primaries to be present in UHECR, the most probable fractions of these primaries were inferred in [5]. The measured distributions of X_{\max} were compared with X_{\max} distributions by combining MC distributions of the assumed primaries. Large differences in the results were found among the hadronic interaction models. Also, a degeneracy of solutions with similar probability can be expected as, generally, there are many combinations of MC distributions of the individual primaries which describe the measured distributions similarly well.

Whereas the fluorescence technique measures the longitudinal profile of the electromagnetic component of the shower, a measurement of the number of muons on the ground (N_μ) can provide an independent way to infer the mass composition of UHECR. Muon detectors have a 100% duty cycle and, when a good resolution of N_μ is achieved ($\lesssim 10\%$), even better separability of the individual primaries can be achieved than in the case of the fluorescence technique. However, there is a lack of N_μ in MC simulations when compared with the measured data [6, 7, 8]. The underestimation of muon production is usually characterized in terms of a muon rescaling factor. Moreover, a stronger relationship between N_μ and the shower energy than between X_{\max} and the shower energy [9] makes the situation more difficult and an independent measurement of the shower energy is needed for composition studies using N_μ . Therefore a simple comparison of the measured distributions of muons with MC predictions would be complicated.

A combined measurement of UHECR showers with the fluorescence technique (X_{\max} and shower energy) and muon detectors (N_μ) could be a more successful way to determine the mass composition of UHECR. In the previous studies, the detected muon and electromagnetic signals were utilized to determine the average mass number of a set of air showers, see e.g. [10]. There are also methods estimating the spread of masses in the UHECR primary beams via correlation of N_μ and X_{\max} [11] or from signals in muon and electromagnetic detectors [12]. However, it needs to be mentioned that the two currently operating experiments do not yet directly measure the muonic component for showers with zenith angles below 60° .

Here we present another method to determine the fractions of the assumed primaries in which the rescaling of N_μ (R_μ) can be achieved simultaneously with a single fit of a combined measurement of X_{\max} and N_μ . For this purpose we use MC showers generated with two hadronic interaction models tuned to the LHC data (run I-II).

In the next section, the generated showers that were used in this work are described. The method to determine the fractions of the assumed primaries and R_μ is introduced in Section 3.

Section 4 contains applications of the method on several examples, testing its performance. The work is summarized in the last section.

2. Simulated Showers

For this work we have simulated $\sim 10^5$ showers with the CONEX 4.37 generator [13, 14] for p and Fe primaries with fixed energy $10^{18.5}$ eV and for each of the two hadronic interaction models (QGSJet II-04 [15] and EPOS-LHC [16, 17]). The zenith angles (Θ) of showers were distributed uniformly in $\cos^2 \Theta$ for Θ in $< 0, 60^\circ >$.

Muons with threshold energy 300 MeV at ~ 1400 m a.s.l. were included to calculate N_μ . Electromagnetic particles of energies above 1 MeV formed the longitudinal profile (dependence of the deposited energy on the atmospheric depth), from which X_{\max} was fitted with the Gaisser-Hillas function by the program CONEX.

For each shower we used Gaussian smearing of X_{\max} and N_μ with a variance equal to $\sigma(X_{\max})$ and $\sigma(N_\mu)$, respectively. These smearings imitate the detector resolutions. We adopted a correction for the attenuation of N_μ with zenith angle due to the different amount of atmosphere penetrated by the air shower before it reaches the ground. The correction was made using a polynomial of 3rd order in $\cos^2 \Theta$ for each model of hadronic interactions. An equally mixed composition of p and Fe was considered for this purpose.

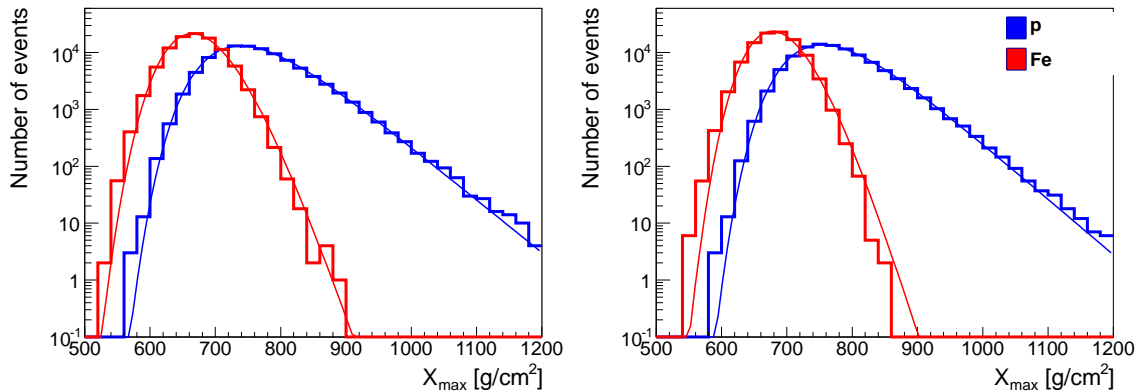


Figure 1: Distributions of X_{\max} parametrized with Gumbel functions g_i . Showers initiated with p (blue) and Fe (red) primaries were simulated with QGSJet II-04 (left) and EPOS-LHC (right) for $\sigma(X_{\max}) = 20$ g/cm².

3. Method

For both hadronic interaction models, we parametrized X_{\max} distributions with Gumbel functions [18] g_i (see Fig. 1) for both primaries $i = p, Fe$. We also parametrized the dependence of mean N_μ , $\langle N_\mu \rangle$, on X_{\max} with quadratic functions in X_{\max} denoted as $\langle N_\mu^i \rangle$ (see Fig. 2), again for both primaries. We introduced the rescaling factor R_μ of $\langle N_\mu^i \rangle$ to incorporate into the method

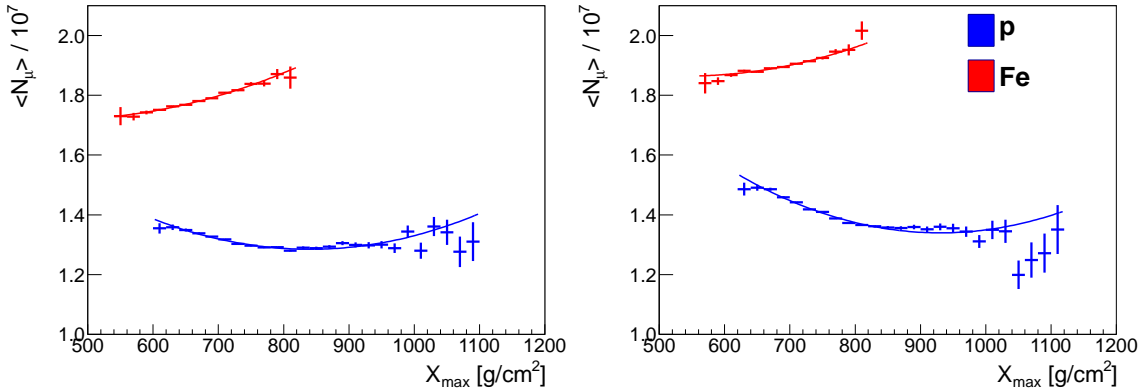


Figure 2: Dependence of mean N_μ on X_{\max} parametrized with quadratic functions $\langle N_\mu^i \rangle$. Showers initiated with p (blue) and Fe (red) primaries were simulated with QGSJet II-04 (left) and EPOS-LHC (right) for $\sigma(X_{\max}) = 20 \text{ g/cm}^2$ and $\sigma(N_\mu)/N_\mu = 10\%$. Only bins of X_{\max} with more than 30 showers were considered in the quadratic fits.

the case when a rescaling of $\langle N_\mu^i \rangle$ obtained from MC is needed to fit the measured $\langle N_\mu \rangle$. Then, for a combination of two primaries with fractions f_i , $\sum f_i = 1$, $\langle N_\mu \rangle$ is given as

$$\langle N_\mu \rangle = \sum_i (w_i \langle N_\mu^i \rangle) R_\mu \quad (3.1)$$

where the weights w_i are expressed as

$$w_i = \frac{f_i \cdot g_i}{\sum_j (f_j \cdot g_j)}. \quad (3.2)$$

For each bin of X_{\max} , $\langle N_\mu \rangle \equiv \langle N_\mu \rangle (X_{\max})$ is calculated as the weighted average of $\langle N_\mu^i \rangle \equiv \langle N_\mu^i \rangle (X_{\max})$ rescaling both $\langle N_\mu^i \rangle$ with the same factor R_μ . The weights $w_i \equiv w_i(X_{\max})$ reflect the relative contribution of each individual primary with relative fraction f_i in each bin of X_{\max} according to $g_i \equiv g_i(X_{\max})$.

Thus, any given dependence of $\langle N_\mu \rangle$ on X_{\max} , which is similar to the dependence of combined proton and iron showers, can be fitted with the two-parameter (f_p and R_μ) fit. The Fe fraction is obtained afterwards as $f_{\text{Fe}} = 1 - f_p$.

An example of application of the method to the mixed composition of showers initiated with 50% p and 50% Fe is shown in Fig. 3. The fitted dependence of $\langle N_\mu \rangle$ on X_{\max} (black points) is shown with the gray dashed line. The hadronic interaction model EPOS-LHC was considered. Starting from the lowest values of X_{\max} , $\langle N_\mu \rangle$ matches $\langle N_\mu^{\text{Fe}} \rangle$ to about 650 g/cm² where a transition towards $\langle N_\mu^{\text{p}} \rangle$ begins. It continues up to about 800 g/cm² where $\langle N_\mu^{\text{Fe}} \rangle$ starts to match $\langle N_\mu^{\text{p}} \rangle$.

4. Application of Method

In this section we show basic examples of the present method and rough estimates how accurately the primary fractions of p and Fe and the muon rescaling factor can be determined. In the

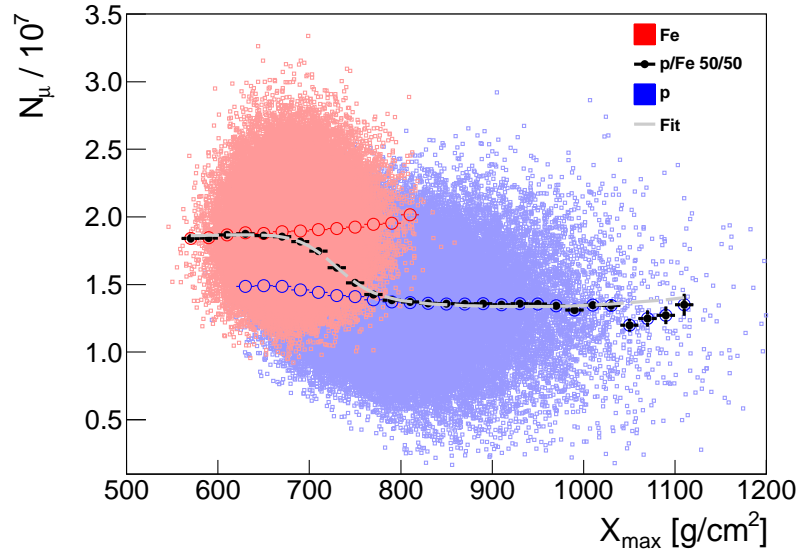


Figure 3: Example of a fit (gray dashed line) for a set of showers composed of 50% p and 50% Fe (black points). Showers were generated with EPOS–LHC for $\sigma(X_{\max}) = 20 \text{ g/cm}^2$ and $\sigma(N_\mu)/N_\mu = 10\%$. The individual p and Fe showers are shown with light blue and light red points, respectively. $\langle N_\mu^p \rangle$ is depicted with blue open points and $\langle N_\mu^{\text{Fe}} \rangle$ with red open points. The fit with g_i and $\langle N_\mu^i \rangle$ parametrized for EPOS–LHC is shown with the gray dashed line.

following, we assumed the detector resolutions to be $\sigma(X_{\max}) = 20 \text{ g/cm}^2$ and $\sigma(N_\mu)/N_\mu = 10\%$. We considered 11 combinations of mixed compositions of p and Fe with fractions in steps of 10% for both hadronic interaction models. Each of these compositions was reconstructed with each of the two parametrizations obtained for the two hadronic interaction models. Additionally, we reconstructed an example dataset with parametrizations of each of the two models to have another assessment of the method with respect to the two models.

On the left panel of Fig. 4, a comparison of the fitted and the true proton fraction is shown for QGSJet II–04 (blue) and EPOS–LHC (red). The reconstructed f_p of showers generated with a different model than that used for the parametrization of g_i and $\langle N_\mu^i \rangle$ are depicted by open black markers. Scenario 1 (2) corresponds to showers produced with QGSJet II–04 (EPOS–LHC) and fitted with the parametrizations obtained from EPOS–LHC (QGSJet II–04) showers.

When the same hadronic interaction model is used for the generation of showers and parametrization of g_i and $\langle N_\mu^i \rangle$, the proton fraction is reconstructed within a few % of the true value. However, in cases of Scenario 1 and 2, the difference between the fitted and the true proton fraction increases with the spread of primary masses of the selected composition. It reaches values up to $\sim 20\%$.

On the right panel of Fig. 4, the muon rescaling is plotted for different true proton fractions. The rescaling factor is found to be within a few % to 1 (precision of the method), when the same models were used for parametrization and generation (red and blue). Black points correspond to the relative difference of N_μ for showers generated with QGSJet II–04 and EPOS–LHC, which is about 6%.

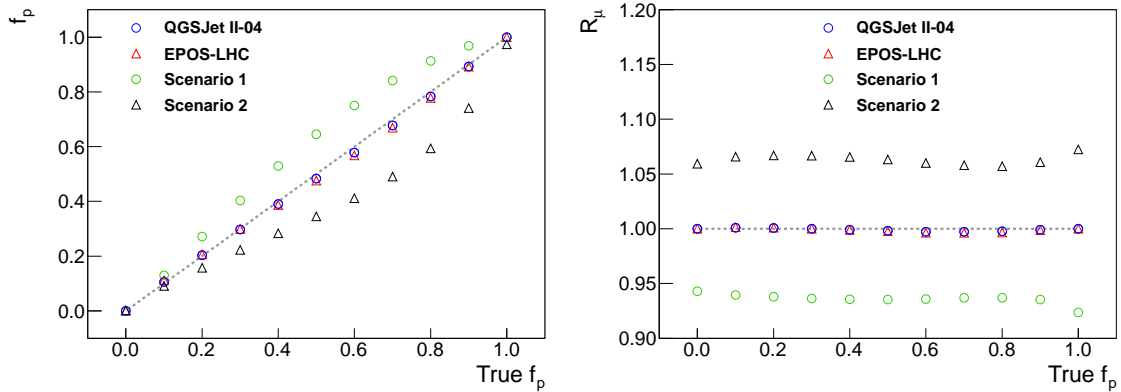


Figure 4: Left panel: Comparison of fitted (f_p) and true proton fraction (True f_p). Right panel: Rescaling of N_μ depending on the true proton fraction. Perfect matches between fitted and true values are shown with dotted gray lines. Smearing with $\sigma(X_{\max}) = 20 \text{ g/cm}^2$ and $\sigma(N_\mu)/N_\mu = 10\%$ was considered. Scenario 1 (2) corresponds to QGSJet II-04 (EPOS-LHC) showers fitted with parametrizations of g_i and $\langle N_\mu^i \rangle$ from EPOS-LHC (QGSJet II-04).

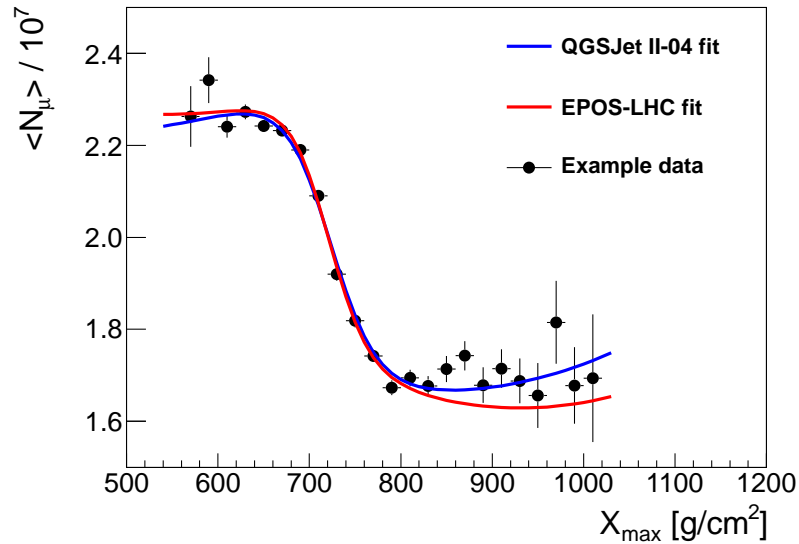


Figure 5: An example of data (black points) fitted with QGSJet II-04 (blue) and EPOS-LHC (red) parametrizations.

As another check, we created example data from 5000 p and 5000 Fe showers produced with QGSJet II-04. For each shower, we scaled N_μ by a factor 1.3 and increased X_{\max} by 7 g/cm^2 . Note that EPOS-LHC generates showers with deeper X_{\max} than QGSJet II-04 by about 14 g/cm^2 on average. These example data were fitted with parametrizations of both models (see Fig. 5). Both fits describe the example data similarly well giving different proton fractions and muon rescaling factors that are shown in Tab. 1. The difference of f_p is about 15% when different parameterizations (Figs. 1,2) based on two most recent models are used. The ratio of R_μ for the two models reflects

again that EPOS–LHC produces about 6% more muons than QGSJet II–04 on average.

Table 1: Fitted parameters for example data.

Model	f_p [%]	R_μ
QGSJet II–04	41 ± 2	1.297 ± 0.004
EPOS–LHC	56 ± 2	1.216 ± 0.004

5. Conclusions

A method of simultaneously obtaining the primary fractions and the muon rescaling factor from X_{\max} and N_μ of UHECR was presented. Simulated showers with two models of hadronic interactions tuned to LHC data (run I-II) were used. The precision of the method was tested with different combinations of p and Fe primaries and with example data. The primary fractions and the muon rescaling factor can be determined within a few %. The difference of the proton fraction reconstructed with the two parameterizations based on the two models of hadronic interactions was observed below 20%. The muon rescaling factor reflected the relative difference (around 6%) in the average muon shower size of the two models of hadronic interactions.

Acknowledgements

This work is funded by the Czech Science Foundation grant 14-17501S.

References

- [1] A. Aab et al. (The Pierre Auger Collaboration), *Phys. Rev. D* **90** (2014) 122005.
- [2] R. U. Abbasi et al. (Telescope Array Collaboration), *Astropart. Phys.* **64** (2014) 49-62.
- [3] J. Abraham et al. (The Pierre Auger Collaboration), *Phys. Rev. Lett.* **101** (2008) 061101.
- [4] T. Abu-Zayyad et al. (Telescope Array Collaboration), *ApJ* **768** (2013) L1.
- [5] A. Aab et al. (The Pierre Auger Collaboration), *Phys. Rev. D* **90** (2014) 122006.
- [6] A. Aab et al. (The Pierre Auger Collaboration), *JCAP* **8** (2014) 019.
- [7] B. Kegl for the Pierre Auger Collaboration, *Proc. of the 33rd ICRC 2013*, arXiv:1307.5059 [astro-ph.HE].
- [8] G. R. Farrar for the Pierre Auger Collaboration, *Proc. of the 33rd ICRC 2013*, arXiv:1307.5059 [astro-ph.HE].
- [9] J. Mathews, *Astropart. Phys.* **22** (2005) 387-397.
- [10] P. Luczak et al., *Proc. of the 33rd ICRC 2013*, arXiv:1308.2059 [astro-ph.HE].
- [11] P. Younk & M. Risse, *Astropart. Phys.* **35** (2012) 807-812.
- [12] J. Vicha et al., *Astropart. Phys.* **69** (2015) 11-17.

- [13] T. Bergmann et al., *Astropart. Phys.* **26** (2007) 420-432.
- [14] T. Pierog et al., *Nucl. Phys. B. - Proc. Suppl.* **151** (2006) 159-162.
- [15] S. S. Ostapchenko, *Phys. Rev. D* **83** (2011) 014018.
- [16] K. Werner, F. M. Liu and T. Pierog, *Phys. Rev. C* **74** (2006) 044902.
- [17] T. Pierog and K. Werner, *Nucl. Phys. B - Proc. Suppl.* **196** (2009) 102-105.
- [18] E. J. Gumbel, *Statistics of extremes*, Dover Publications (2004).